ESTIMATIONS OF SEDIMENT TRANSPORT IN A GULLY SYSTEM USING THE MORPHOLOGICAL METHOD

Wen Dai[1], Jiaxin Fan[2], Aili Liu[1], Chun Wang[1,2,3], Weitao Li[2,3], Min Li[3], Xi Chen[3], Chengyi Zhao[1] *

[1] School of Geographical Sciences, Nanjing University of Information Science & Technology, Nanjing 210044, China;
- (wen.dai, liuaili, zhaocy)@nuist.edu.cn
[2] School of Remote Sensing & Geomatics Engineering, Nanjing University of Information Science & Technology, Nanjing 210044, China; - fanjx1998@163.com
[3] School of Geographical Information and Tourism, Chuzhou University, Chuzhou 239000, China
- (chenxi_njnu, wangchun93)@126.com, limin2652035@163.com, liweitao_801225@chzu.edu.com

Commission IV, WG IV/3

KEY WORDS: Sediment Transport, Topographic Changes, Sediment Budgets, Loess Catchments, DEMs of difference.

ABSTRACT:

Gully erosion seriously threatens farmland and causes soil loss. Estimating sediment transport in a gully system is important for understanding the mechanisms of gully erosion. The morphological method successfully applied in estimating bed-material transport in rivers, for some decades, has yet to be applied to gully erosion. Here, we estimate sediment transport in a gully system using the morphological method. It was applied to a laboratory simulation of a loess catchment. Nine high-resolution Digital Elevation Models (DEMs) were acquired by digital close-range photogrammetry and used to determine morphological change. Mass conservation was used to explain measured morphological change, and to infer the changes in sediment transport in space. The results showed that gully erosion is greater than deposition in the initial stages of gully development. Serious gully erosion occurs in the gully heads or upstream areas, and the erosion and deposition become balance in the downstream area. A large proportion of the total transport was actually concentrated into one main channel. Meanwhile, the active areas (high transport) of sediment transport gradually developed from the downstream to upstream with the gully development.

1. INTRODUCTION

Gully erosion, which widely threatens farmland and the environment (Poesen et al., 2003), is the main source of sediment at the catchment scale in many circumstances (Valentin et al., 2005). In the loess plateau of China, gully erosion contributes to between 60% and 70% of all eroded sediment (Dai et al., 2020; Li et al., 2003). Estimating sediment transport in a gully system is important for understanding the mechanisms of gully erosion.

A number of soil erosion models including gully erosion for estimating sediment transport at the hillslope and catchment scales have been proposed, for some decades (Alonso et al., 1981; De Roo et al., 1996; Govers, 1992; Wu et al., 2016). Although these models allow estimation of sediment budgets and sediment transport capacities, and provided the sediment supply condition is properly determined, sediment transport rates, they have considerable uncertainty and can be highly demanding in terms of input data and data for calibration (Mahmoodabadi et al., 2014; Zhang et al., 2008).

A possible alternative is to infer spatial patterns of sediment transport from morphological change through time, named the 'morphological method' (Ashmore & Church, 1998; S. Lane et al., 1994). This is appealing because it is becoming increasingly easy to measure topography repeatedly to a high resolution and precision (Dai et al., 2021; Dai et al., 2019).

The morphological method uses mass conservation to explain measured morphological change, and to infer the changes in sediment transport in space (Vericat et al., 2017). Research has shown that the morphological method is feasible for inferring bed-material transport rates in braided streams (Antoniazza et al., 2019; Ashmore & Church, 1998; S. Lane et al., 1995; Vericat et al., 2017). It has also been applied to hillslope sediment yield estimation (Heckmann & Vericat, 2018). However, it has yet to be applied to gully erosion and deposition. In this work, the objective is to estimate sediment transport in a gully system in both one-dimension (1-D) and two-dimensions (2-D) using the morphological method. The focus is upon laboratory-simulated loess catchments as these allow for optimal control of data acquisition.

2. METHODOLOGY

2.1 Area And Data

Here, we focus on a laboratory loess catchment, constructed in the rainfall erosion test facility at the State Key Laboratory of Soil Erosion and Dryland Farming on the Loess Plateau, China (Figure 1). The catchment covers an area of 31.5 m^2, with a maximum length of 9.1 m, maximum width of 5.8 m, circumference of 23.3 m and valley height difference of 3.15 m. This catchment was filled with loess of bulk density 1.39 g/cm^3. Considering that rainfall is the key factor for driving gully erosion, we simulated 25 rainfalls on the catchment.

* Corresponding author

During the simulation, nine sets of DEMs were acquired by digital close-range photogrammetry. We evenly distributed 18 control points and 20 check points in the study area and employed an independent coordinate system to survey the control and check points. The horizontal and vertical root mean square error (RMSE) of these points were less than 0.3 mm. Then, we used the control points to correct the photogrammetry process, and the check points to access the errors of the generated 10-mm DEMs. The horizontal and vertical RMSE of the generated DEMs were 1.5 mm, and 2 mm, respectively.

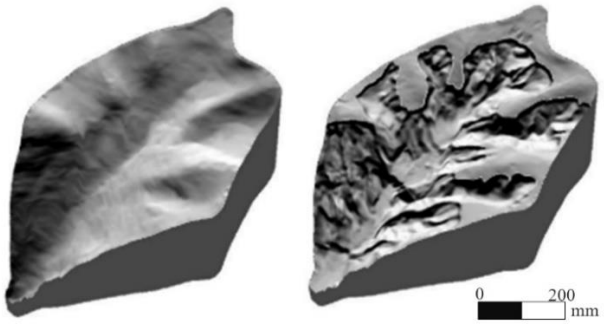

Figure 1. study area. left and right are 1st and 9th DEM, respectively.

2.2 Change Detection

With the repeated survey in the study area, the morphological changes can be easily observed from DEMs of difference (DoD). We subtracted the second DEM from the first DEM in every survey such that positive change represented erosion and therefore a contribution to sediment transport; and negative change deposition and a loss of sediment transport. However, errors always exist in DEMs. Before calculating DoDs, DEM error should be propagated into the corresponding DoDs (Anderson, 2019). Thus, a 95% confidence level Student's t test was applied to threshold the measured DoDs. Only the cells with change outside the t-test thresholds was regard as real topographic change. At the 95% confidence, and under the assumption that the errors were independent, random and Gaussian, the thresholds were defined as (Brasington et al., 2003; S. N. Lane et al., 2003):

$$t = \pm 1.96\sqrt{{E_a}^2 + {E_b}^2} \quad (1)$$

where t = threshold
E_a = vertical precisions of DEM a
E_b = vertical precisions of DEM b

2.3 Morphological Method

The morphological method is based on mass conservation, in which geomorphological changes can be linked to sediment transport. The equation of this method is as follow(Antoniazza et al., 2019; Exner, 1925):

$$\left(\frac{\partial Q_b^x}{\partial x}\right) + \left(\frac{\partial Q_b^y}{\partial y}\right) + (1-p) \times \left(\frac{\partial Z_{xy}}{\partial t}\right) + \left(\frac{\partial C_b}{\partial t}\right) = 0 \quad (2)$$

where Q_b = the sediment transport in the x and y downstream and cross-stream directions respectively
p = sediment porosity
Z = elevation in position (x, y)
t = time
C_b = the concentration per unit bed area of sediment in motion

By neglecting the lateral overbank sediment transport, and assuming that C_b is constant in space and time, Equation (1) becomes in one-dimension (Vericat et al., 2017):

$$\left(\frac{\partial Q_b}{\partial x}\right) + (1-p) \times \left(\frac{\partial Z}{\partial t}\right) = 0 \quad (3)$$

where Q_b = the cross-sectionally averaged sediment transport rate
Z = the cross-sectionally averaged morphological change.

For one-dimension application of the method, net volume changes per cross-section are measured by DEM differencing. Then, cross-section volume changes are routed from cross-section to cross-section. The route starts from the most upstream cross section because the fluxes of the most upstream cross section is zero within a complete catchment. Then, Equation (2) can be discretized as:

$$S_j = S_{j-1} - \left(\frac{\sum \rho(1-p)\Delta V_j}{t}\right) \quad (4)$$

where S_j = the transport for a given cross section j
S_{j-1} = the transport rate coming from the upstream cross-section
ρ = the material density
p = the porosity
ΔV_j = the net volume change by cross-section measured by DEM differencing
t = the duration time.

For application of the morphological method in two-dimensions in DEMs, discretization application of Equation (2) at pixel level is needed. Figure 2 shows the principle of mass conservation at pixel level. For each cell, the sum of the sediment received from upstream surrounding cells and the topographic changes (erosion or deposition) within the cell should be equal to the sum of the sediment transported to the downstream cells.

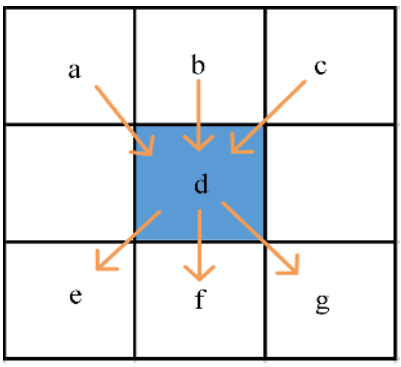

a + b + c + d = e + f + g

Figure 2. the principle of mass conservation at pixel level.

According to Figure 2, for application of the morphological method in two-dimensions, cell-by-cell sediment routing is required (S. Lane et al., 1995). Here, we use a multiple flow direction model (Holmgren, 1994) to route the sediment transport.

Each cell receives a certain volume of sediment from surrounding cells that are higher in altitude, Q_s. It then supplies sediment to cells that are lower in altitude in proportion to their slope via a Holmgren (1994) type function. Hence, the sediment transport in any direction k, Q_b^k, is defined as:

$$Q_b^k = \left(\frac{tan\ s_k}{\sum_1^8 tan\ s_k}\right)^{\alpha} \times \left[Q_s + \rho(1-p)\Delta V_{ij}\right] \qquad (5)$$

where k = the index of each of the 8 surrounding cells that could deliver sediment to cell ij if they have positive slopes
s_k = the slope of the surrounding cells k
α = the parameter that controls the degree of flow diffusion (or concentration) which tends to a classic D8 algorithm as α tends to infinity, and tends to multiple routing as α is 1.

The Holmgren flow routing was applied in the TopoToolBox system (Schwanghart & Kuhn, 2010). For two-dimensions application of the Holmgren flow routing, the α that controls the degree of flow diffusion (or concentration), is required. Here, we used a Monte Carlo model to determine the best value. We randomly selected the value of α from [1, 10] 200 times and used the negative transport condition to evaluate the performance.

Given mass conservation, the sediment transport should not be negative. If negative transport occurs, there is more sediment being deposited than supplied. Thus, the extent of negative transport is an index of the quality of the calculation and we use it here to assess processing options, notably the choice of DEM for routing. In this case, the routing could be applied to the DEM at the start of each calculation period, the DEM at the end of each period or the average of the two. The sediment transport routing in 2-D depends on which DEM was used. Then, we compared the initial DEM, final DEM, and the average of initial and finial DEM for routing sediment transport in every survey period.

3. RESULTS AND DISCUSSION

3.1 Morphological Changes And 1-D Sediment Transport

The eight DoDs calculated from the nine available DEMs are shown in Figure 3, after application of the detection threshold. The erosion patches (red) upon the gully heads and gully margins. Deposition patches (blue) without a clear spatial pattern can be noted anywhere within gully area. However, deposition and erosion patches can also be seen within the same cross section. This will lead to erosion and deposition within a cross section cancelling itself out, which affects 1-D application of the morphological method.

Figure 4 shows the results from the 1-D morphological method. In the first four periods, the sediment transport always increases from upstream to downstream, which means that the gully erosion is greater than deposition in the initial stages of gully development, as the gullies erode headward. In the latter four periods, the sediment transport increased at first and then became stable at a certain level. Serious gully erosion continued in the gully heads, but erosion and deposition became more balanced downstream.

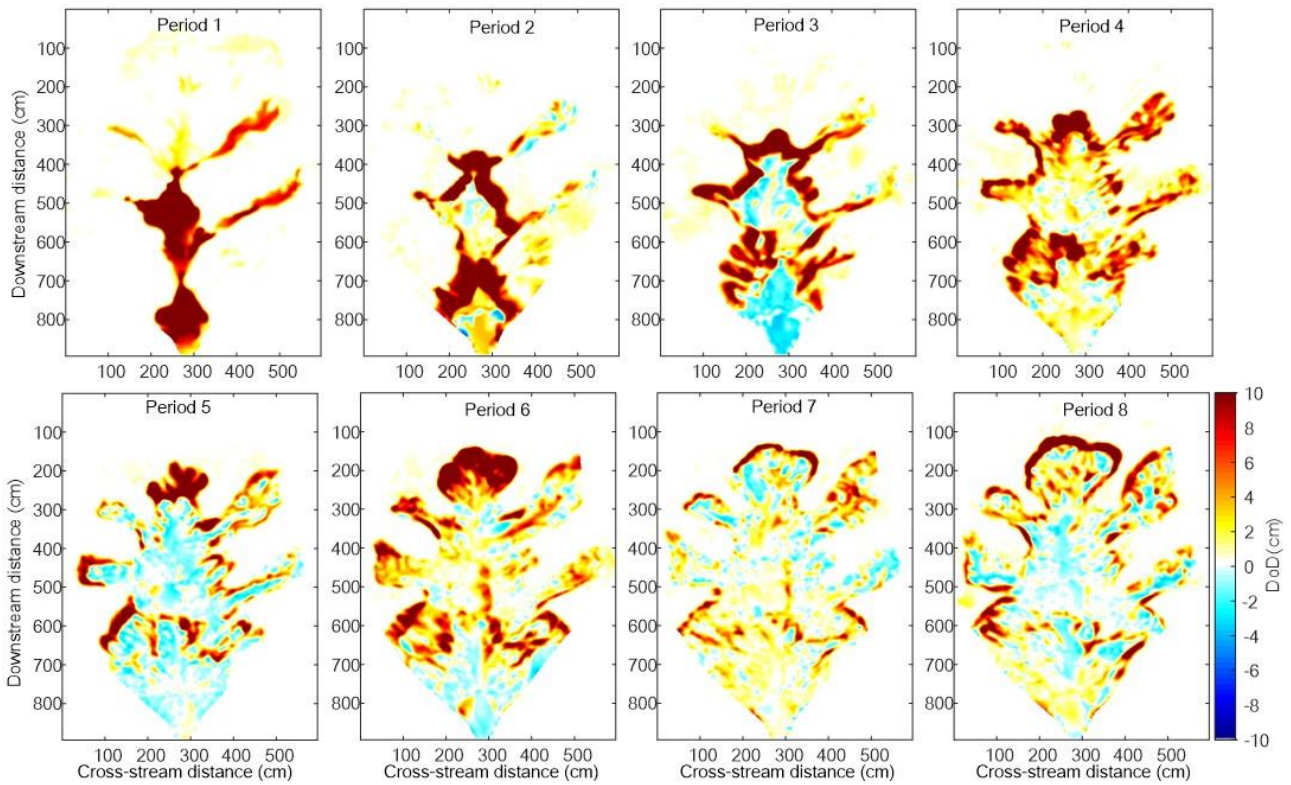

Figure 3. morphological changes of the nine surveys.

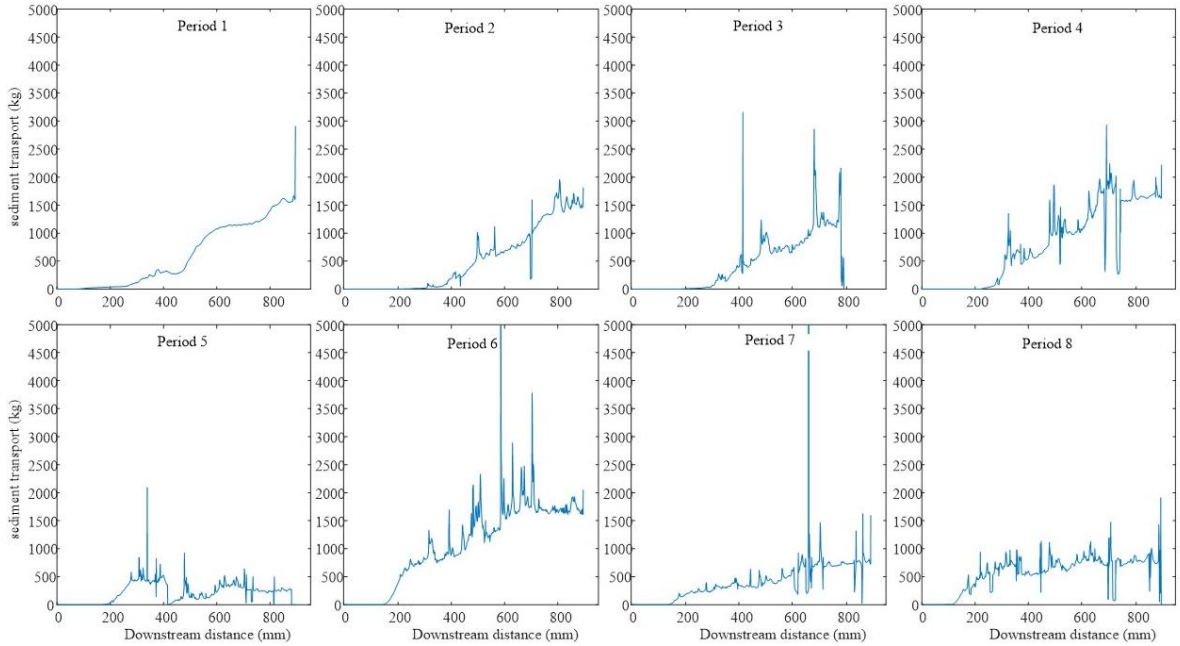

Figure 4. 1-D sediment transport.

3.2 2-D Sediment Transport

Figure 5 shows the effects of α on negative transport. 200 times Monte Carlo experiments were performed on the Period 2. With the increase of α , the negative transport extent remains small but grows. Especially, when α is 1, the negative transport is the lowest. Thus, we used the α of 1 for next experiments.

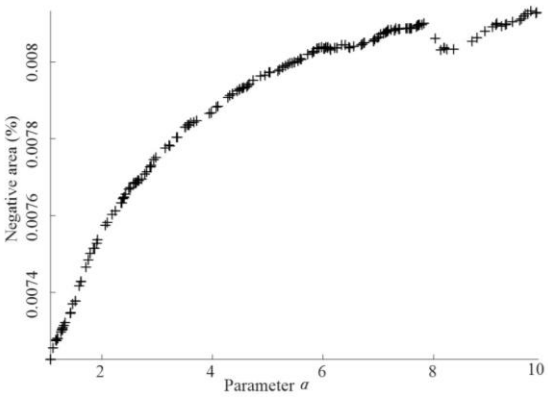

Figure 5. comparison the use of diffrent α.

Figure 6 compares the effects of DEM choice (initial, average or final) on the extent of negative transport. The latter always was always lowest for the initial DEMs. Therefore, the initial DEMs in every survey period were used for sediment routing. Figure 6 also shows that the negative transport extent remains small but grows through time. This extent is likely to be over-estimated as with the routing applied in this calculation, negative transport is routed. Thus, once one cell's transport becomes negative, this will be propagated to surrounding cells until there is enough erosion to counter it. This is likely to be a result of errors in routing, and notably the fact that as the gully system develops the extent of channel routing increases. Channel routing is less likely to be topographically controlled and more likely to be hydraulically controlled and the failure to represent the latter correctly is likely to be why there are zones where deposition is greater than available sediment supply.

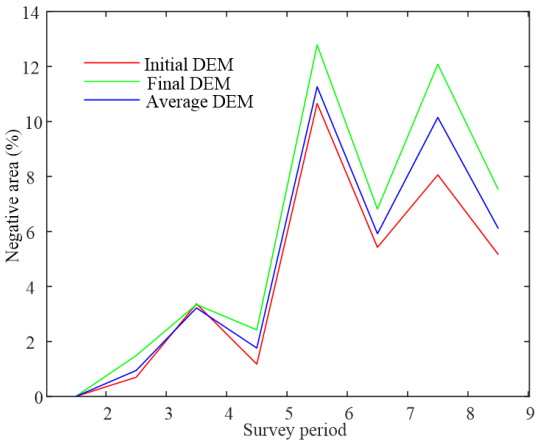

Figure 6. comparison the use of initial, final, and average DEM.

The negative transport would be related to the amount of deposition. Figure 7 shows the relation between deposition and the negative transport in the eight periods. The negative transport increase with the proportion of deposition in each period. This confirms that once one cell's transport becomes negative, this will be propagated to surrounding cells until there is enough erosion to counter it.

Figure 8 shows the results of 2-D morphological method. Gully erosion was the main source that caused sediment in this catchment. All sediment transport was concentrated in the gully network. A large proportion of the total transport was actually concentrated into one main channel. However, the active areas (high transport) of sediment transport gradually developed from the downstream to upstream with the gully development. The lower part (600 – 900 mm) of the catchment was much active in the first period and became less active in the latter period. The

upper part (100 – 400 mm) of the catchment became more and more active from the first to the final period.

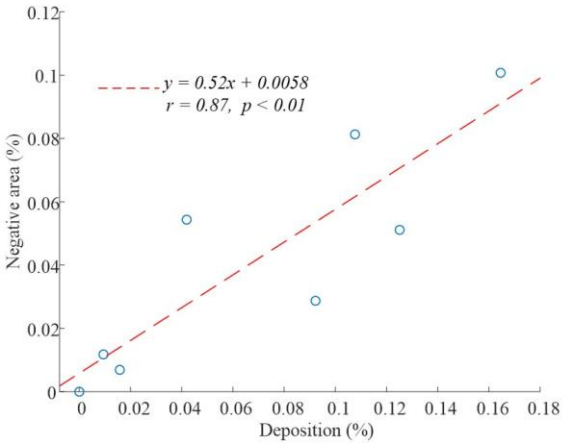

Figure 7. the relation between negative transport and deposition.

4. CONCLUSIONS

In conclusion, we estimated sediment transport in a gully system in both 1-D and 2-D using the morphological method. The results show that: (1) gully erosion is greater than deposition in the initial stages of gully development; (2) serious gully erosion continues in the gully heads or upstream areas, and the erosion and deposition becomes balanced in the downstream area in later periods; and (3) a large proportion of the total transport was actually concentrated into one main channel; and (4) the active areas of sediment transport gradually developed from the downstream to upstream with the gully development.

ACKNOWLEDGEMENTS

We are grateful for the financial support from the National Natural Science Foundation of China (grant numbers 42130405, 41930102, and 42171402) and the Key Project of Provincial Natural Science Research Plan of Anhui Universities (Grant No. KJ2021ZD0130), and The Startup Foundation for Introducing Talent of NUIST (2022r019).

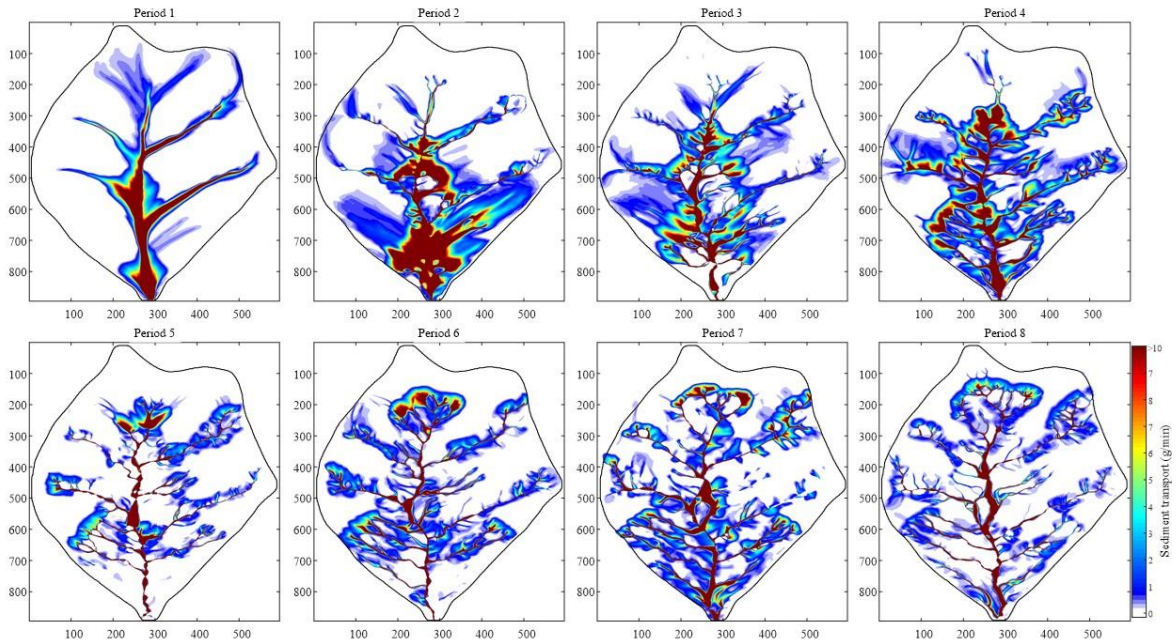

Figure 8. 2-D sediment transport.

REFERENCES

Alonso, C., Neibling, W., & Foster, G. 1981. Estimating sediment transport capacity in watershed modeling. *Transactions of the ASAE, 24*(5), 1211-1220.

Anderson, S. W. 2019. Uncertainty in quantitative analyses of topographic change: error propagation and the role of thresholding. *Earth surface processes and landforms, 44*(5), 1015-1033. doi:10.1002/esp.4551

Antoniazza, G., Bakker, M., & Lane, S. N. 2019. Revisiting the morphological method in two - dimensions to quantify bed - material transport in braided rivers. *Earth surface processes and landforms, 44*(11), 2251-2267. doi:10.1002/esp.4633

Ashmore, P., & Church, M. 1998. Sediment transport and river morphology: a paradigm for study. *Gravel-bed Rivers in the Environment*, 115-148.

Brasington, J., Langham, J., & Rumsby, B. 2003. Methodological sensitivity of morphometric estimates of coarse fluvial sediment transport. *Geomorphology, 53*(3-4), 299-316. doi:10.1016/s0169-555x(02)00320-3

Dai, W., Hu, G.-h., Yang, X., Yang, X.-w., Cheng, Y.-h., Xiong, L.-y., Strobl, J., & Tang, G.-a. 2020. Identifying ephemeral

gullies from high-resolution images and DEMs using flow-directional detection. *Journal of Mountain Science, 17*(12), 3024-3038. doi:10.1007/s11629-020-6084-5

Dai, W., Xiong, L., Antoniazza, G., Tang, G., & Lane, S. N. 2021. Quantifying the spatial distribution of sediment transport in an experimental gully system using the morphological method. *Earth surface processes and landforms, 46*(6), 1188-1208. doi:10.1002/esp.5094

Dai, W., Yang, X., Na, J., Li, J., Brus, D., Xiong, L., Tang, G., & Huang, X. 2019. Effects of DEM resolution on the accuracy of gully maps in loess hilly areas. *Catena, 177*, 114-125. doi:10.1016/j.catena.2019.02.010

De Roo, A., Wesseling, C., & Ritsema, C. 1996. LISEM: a single‐event physically based hydrological and soil erosion model for drainage basins. I: theory, input and output. *Hydrological processes, 10*(8), 1107-1117.

Exner, F. M. 1925. Uber die wechselwirkung zwischen wasser und geschiebe in flussen. *Akad. Wiss. Wien Math. Naturwiss. Klasse, 134*(2a), 165-204.

Govers, G. 1992. *Evaluation of transporting capacity formulae for overland flow conditions*. London: University College London Press.

Heckmann, T., & Vericat, D. 2018. Computing spatially distributed sediment delivery ratios: inferring functional sediment connectivity from repeat high-resolution digital elevation models. *Earth surface processes and landforms, 43*(7), 1547-1554. doi:10.1002/esp.4334

Holmgren, P. 1994. Multiple flow direction algorithms for runoff modelling in grid based elevation models: an empirical evaluation. *Hydrological processes, 8*(4), 327-334.

Lane, S., Richards, K., & Chandler, J. 1994. Developments in monitoring and modelling small‐scale river bed topography. *Earth surface processes and landforms, 19*(4), 349-368.

Lane, S., Richards, K., & Chandler, J. 1995. Morphological estimation of the time‐integrated bed load transport rate. *Water Resources Research, 31*(3), 761-772.

Lane, S. N., Westaway, R. M., & Murray Hicks, D. 2003. Estimation of erosion and deposition volumes in a large, gravel-bed, braided river using synoptic remote sensing. *Earth surface processes and landforms, 28*(3), 249-271. doi:10.1002/esp.483

Li, Y., Poesen, J., Yang, J., Fu, B., & Zhang, J. 2003. Evaluating gully erosion using 137Cs and 210Pb/137Cs ratio in a reservoir catchment. *Soil and Tillage Research, 69*(1-2), 107-115.

Mahmoodabadi, M., Ghadiri, H., Rose, C., Yu, B., Rafahi, H., & Rouhipour, H. 2014. Evaluation of GUEST and WEPP with a new approach for the determination of sediment transport capacity. *Journal of Hydrology, 513*, 413-421.

Poesen, J., Nachtergaele, J., Verstraeten, G., & Valentin, C. 2003. Gully erosion and environmental change: importance and research needs. *Catena, 50*(2–4), 91-133.

Schwanghart, W., & Kuhn, N. J. 2010. TopoToolbox: A set of Matlab functions for topographic analysis. *Environmental Modelling & Software, 25*(6), 770-781. doi:10.1016/j.envsoft.2009.12.002

Valentin, C., Poesen, J., & Li, Y. 2005. Gully erosion: Impacts, factors and control. *Catena, 63*(2-3), 132-153. doi:10.1016/j.catena.2005.06.001

Vericat, D., Wheaton, J. M., & Brasington, J. 2017. Revisiting the Morphological Approach: Opportunities and Challenges with Repeat High- Resolution Topography. *Gravel-Bed Rivers: Process and Disasters*, 121-158. doi:10.1002/9781118971437.ch5

Wu, B., Wang, Z., Shen, N., & Wang, S. 2016. Modelling sediment transport capacity of rill flow for loess sediments on steep slopes. *Catena, 147*, 453-462. doi:10.1016/j.catena.2016.07.030

Zhang, J. X., Chang, K. T., & Wu, J. Q. 2008. Effects of DEM resolution and source on soil erosion modelling: a case study using the WEPP model. *International Journal of Geographical Information Science, 22*(8), 925-942.